INTERNATIONAL CENTER FOR NUMERICAL METHODS IN ENGINEERING

Finite Volume vs Finite Element Is There Really a Choice?

O. C. Zienkiewicz
E. Oñate

Publication, CIMNE Nº 8, November 1990

Finite Volume vs Finite Element
Is There Really a Choice?

O. C. Zienkiewicz
E. Oñate

E.T.S. de Ingenieros de Caminos, Canales y Puertos
Universidad Politécnica de Cataluña, Barcelona

Paper published in the book commemorating Prof. E. Stein's 60th anniversary.
"Non linear Computational Mechanics-State of the Art"
Editors, P.Wriggers and W. Wagner, Springer-Verlag 1991

Publication CIMNE Nº-8, Noviembre 1990

International Center for Numerical Methods in Engineering
Gran Capitán s/n, 08034 Barcelona, Spain

FINITE VOLUMES VS FINITE ELEMENTS. IS THERE REALLY A CHOICE ?

O.C. ZIENKIEWICZ †
University College of Swansea, U.K.

and

E. OÑATE
†† Universitat Politecnica de Catalunya
08034 Barcelona, Spain

Summary

The finite volume method appears to be a particular case of finite elements with a non Galerkin weighting. It is of course less accurate for self adjoint problems but has some computationally useful features for first order equations involving only surface integrals. For certain problems this is a substational economy and leads to computationaly useful approximations.

Introduction

The finite volume method evolved in the early seventies via finite difference approximation and today has many proponents in the field of fluid mechanics (Mc Donald [1], Mc. Cormack and Paullay [2], Rizzi and Inouye [3], Patankar [4]). In the field of CSM (Computational Solid Mechanics) it appears to has been introduced by Wilkins [5] as an alternative approximation to derivatives in a *cell*. In this he defines the average gradient of an arbitrary function u in a volume Ω as

$$\left(\frac{\partial u}{\partial x_i}\right)_{av.} \equiv \frac{1}{\Omega}\int_\Omega \frac{\partial u}{\partial x_i} d\Omega = \frac{1}{\Omega}\oint_s u n_i ds \tag{1}$$

using the well known divergence theorem.

Such definition of gradients can be written entirely in terms of function values at the boundaries of a volume and has been used in the early "hydrocodes" of Lawrence Livermore Laboratory.

A comprehensive description of the finite volume techniques is given by Hirsch [6] and lists their apparent merits viz a viz finite element and finite difference approximations. Amongst these he considers as particularly important:

(i) the conservation of fluxes $F = F(u)$ in a *control volume* when the procedure is applied to such conservation equation as

$$\frac{\partial u}{\partial t} + \frac{\partial F_i}{\partial x_i} \equiv \frac{\partial u}{\partial t} + \nabla^T \mathbf{F} = Q \tag{2}$$

(ii) The ease of applying natural (flux) boundary conditions.

In this note we shall show that the above features exist in the general finite element process and that they do not distinguish in any way to the finite volume method. Further, in problems of self-adjoint operators in which

---

† Currently holding Unesco Chair of Numerical Methods in Engineering at ††

$$F_i = F_i(\frac{\partial u}{\partial x_j}) = -k_{ij}\frac{\partial u}{\partial x_j} \tag{3}$$

it is well known that the finite element method when used with Galerkin weighting provides an optimal approximation and must therefore be, in such cases, more accurate than any alternative.

What then is the distinguishing feature of the finite volume method which can make it attractive?. The answer lies simply in a possible computation advantage of the finite volume procedure in which the major contribution involves only the boundaries of the control volumes. Whether this sole advantage of the finite volume form is sufficient to compensate for a possible accuracy loss, only extensive experiment will show. In the meantime we shall derive below a finite volume format in which a precise interpolation of the variables is used to avoid the fairly arbitrary definitions often used by finite volume proponents.

A General Finite Volume Format

All discrete, generally finite elements, approximations to a differential equation system (such as for instance that of eq (2)) and its boundary conditions can be written for a general equation system.

$$\mathbf{A}\ \mathbf{u} = \mathbf{f} \quad \text{in} \qquad \Omega \tag{4a}$$

and the boundary conditions

$$\mathbf{B}\mathbf{u} = \mathbf{t} \quad \text{in} \quad \Gamma \tag{4b}$$

in a unified format:

1) The independent unknowns are approximated as

$$\mathbf{u} \simeq \hat{\mathbf{u}} = \mathbf{N}_i\bar{\mathbf{u}}_i \qquad (i = 1, \cdots, n) \tag{5}$$

where $\bar{\mathbf{u}}_i$ are the unknown parameters and $\mathbf{N}_i$ are the basis functions.

2) The approximating system of equations is written as a set of *algebraic equations*

$$\int_\Omega \mathbf{W}_j^T(\mathbf{A}\hat{\mathbf{u}} - \mathbf{f})d\Omega + \oint_\Gamma \mathbf{W}_j^T(\mathbf{B}\hat{\mathbf{u}} - \mathbf{t})d\Gamma = 0 \tag{6}$$

where $\mathbf{W}_j^T$ $(j = 1, \cdots, n)$ are weighting functions.

Eq.(6) can be written for linear systems, after substituting of the interpolation (5), as

$$\mathbf{K}\bar{\mathbf{u}} = \mathbf{f} \tag{7}$$

where the usual additive property of element or subdomain contributions is preserved whatever the form of the weighting functions.

In self adjoint problems the optimal weighting is the Galerkin one with

$$\mathbf{W}_j = \mathbf{N}_j \tag{8}$$

This leads to minimum energy norm errors and preserves symmetry of matrix **K** and is the basis of most frequently used finite element procedures. However other weightings can be used recovering all possible approximation methods (viz Zienkiewicz and Taylor [7]). In what follows we shall use standard finite element interpolations $\mathbf{N}_i$ with $\bar{\mathbf{u}}_i$ standing for nodal values in element subdomains.

The finite volume procedure is in fact a special case of the weighted eq.(6) in which

$$\mathbf{W}_j = \mathbf{I} \text{ in } \Omega_c \quad (\text{ and } \mathbf{W}_j = \mathbf{0} \text{ elsewhere}) \tag{9}$$

where **I** is the unity matrix and Ω_c is a control volume which can be prescribed in various ways.

To fix ideas we shall consider a scalar equation with a variable u as given below

$$\frac{\partial u}{\partial t} + \frac{\partial F_k}{\partial x_k} - \frac{\partial}{\partial x_k} k \frac{\partial u}{\partial x_k} \equiv \frac{\partial u}{\partial t} + \nabla^T \mathbf{F} - \nabla^T k \nabla u = Q \tag{10a}$$

This is to be satisfied in a domain Ω with appropiate boundary conditions

$$\begin{aligned} u &= \bar{u} \qquad \text{on} \quad \Gamma_u \\ -k\frac{\partial u}{\partial x_n} &= \bar{q} \qquad \text{on} \quad \Gamma_q \end{aligned} \tag{10b}$$

where $\Gamma = \Gamma_u \cap \Gamma_q$ is the boundary of the domain Ω.

The general approximation can now be written, assuming that $F_i = A_i u$, as

$$M_{ji}\dot{\bar{u}}_i + C_{ji}\bar{u}_i + K_{ji}\bar{u}_i + f_j = 0 \tag{11}$$

in which where after using appropriately the Gauss divergence theorem we have†

$$M_{ji} = \int_{\Omega_j} W_j N_i d\Omega \tag{12a}$$

$$C_{ji} = -\int_{\Omega_j} [\nabla W_j]^T A_k N_i d\Omega + \oint_{\Gamma_j} W_j A_k N_i n_k d\Gamma \tag{12b}$$

$$K_{ji} = \int_{\Omega_j} [\nabla W_j]^T k \nabla N_i d\Omega - \oint_{\Gamma_j} W_j k \frac{\partial N_i}{\partial n} d\Gamma \tag{12c}$$

---

† Note that in (10–11) index k is used for coordinate directions and i, j denotes node numbers. We can write alternatively

$$[\nabla W_j]^T A_k \nabla N_i \equiv W_{j,k} A_k N_{i,k} \quad \text{etc. implying summation in } k$$

$$f_j = \int_{\Omega_j} W_j Q d\Omega \tag{12d}$$

In above Ω_j is the *control volume* associated with variable j (to use the finite volume terminology) where $W_j \neq 0$ and which may include the external boundary Γ of the total domain. Providing both W_j and N_j are so chosen that integrals (12) can be evaluated then whatever the external boundary we can specify on it either the normal fluxes ($-k\frac{\partial u}{\partial x_n} = \bar{q}$) or values of $u = \bar{u}$ with equal ease, using either the Galerkin (eq.(8)) or finite volume (eq.(9)) forms.

To illustrate above consider a field of arbitary triangles with linear interpolations with the control volume for node j shown shaded in Figure 1.

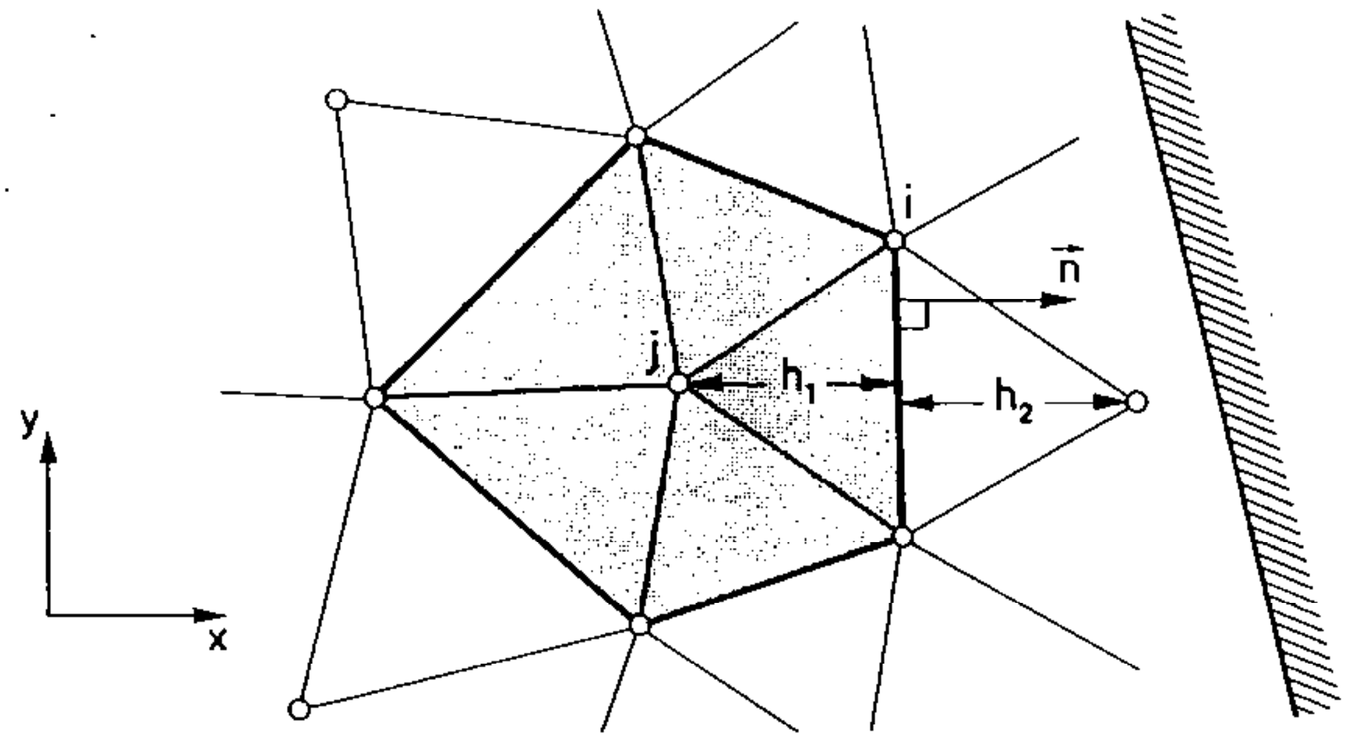

Figure 1. An assembly of finite elements/ finite volumes with shading indicating control volume.

In "standard" finite element assembly the weighting function $W_j = N_j$ is of the form shown in Figure 2a and Ω_j includes all the elements associated with jth node.

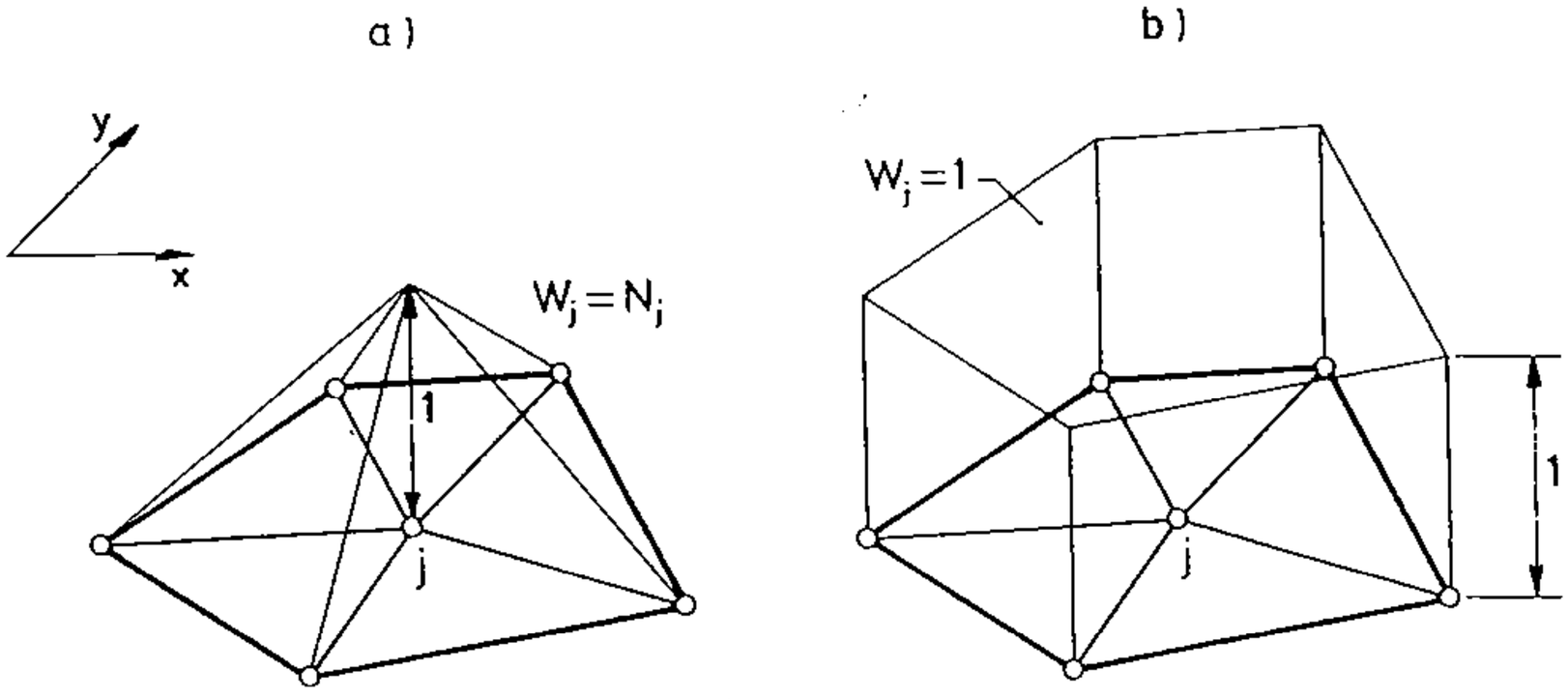

Figure 2. Weighting and basis functions for finite element (a) and finite volume (b)approximations for Figure 1.

As $N_j = 0$ all over the periphery of Ω_j no surface integral exists in expressions for C_{ji} or K_{ji}, thus eliminating the need of evaluating the fluxes on such boundaries. However, on all element interfaces integrals along lines such as $i-j$ (connecting nodes $i-j$) vanish as

$$\left(\int_i^j N_j A_k N_i n_k d\Gamma\right)_{left} = -\left(\int_i^j N_j A_k N_i n_k d\Gamma\right)_{right}$$
$$\left(\int_i^j N_j k \frac{\partial N_i}{\partial n} d\Gamma\right)_{left} = -\left(\int_i^j N_j k \frac{\partial N_i}{\partial n} d\Gamma\right)_{right} \tag{13}$$

for elements left and right of the interface.

This of course means that flux continuity is preserved in a weighted sense. Further direct flux identity on such faces exists in general if we note that on each $N_i + N_j = 1$ with standard interpolations [7]. However, the volume integrals of C_{ji}, K_{ji}, etc. have to be evaluated.

Now if we consider the finite volume situation (Figure 2b) it is evident that all volume (area) integrals dissapear from expressions C_{ji} and K_{ji}. Further the surface integrals in the expression for C_{ji} presents no difficulty in evaluating providing A_k and N_i are continuous in the domain. However inmediately a dificulty arises with the diffusive terms in the K_{ji} integral. Here evaluation of

$$\left(\oint_\Gamma W_j k \frac{\partial N_i}{\partial n} d\Gamma\right) \bar{u}_i$$

presents the difficulty as $\frac{\partial N_i}{\partial n}$ is not continuous.

In the normal direction n as illustrated in Figure 1 between two elements we have a discontinuity shown in Figure 3 with $\frac{\partial N_i}{\partial n}$ jumping from a value of $1/h_1$ to $-1/h_2$ where heights of adjacent triangles are denoted h_1 and h_2.

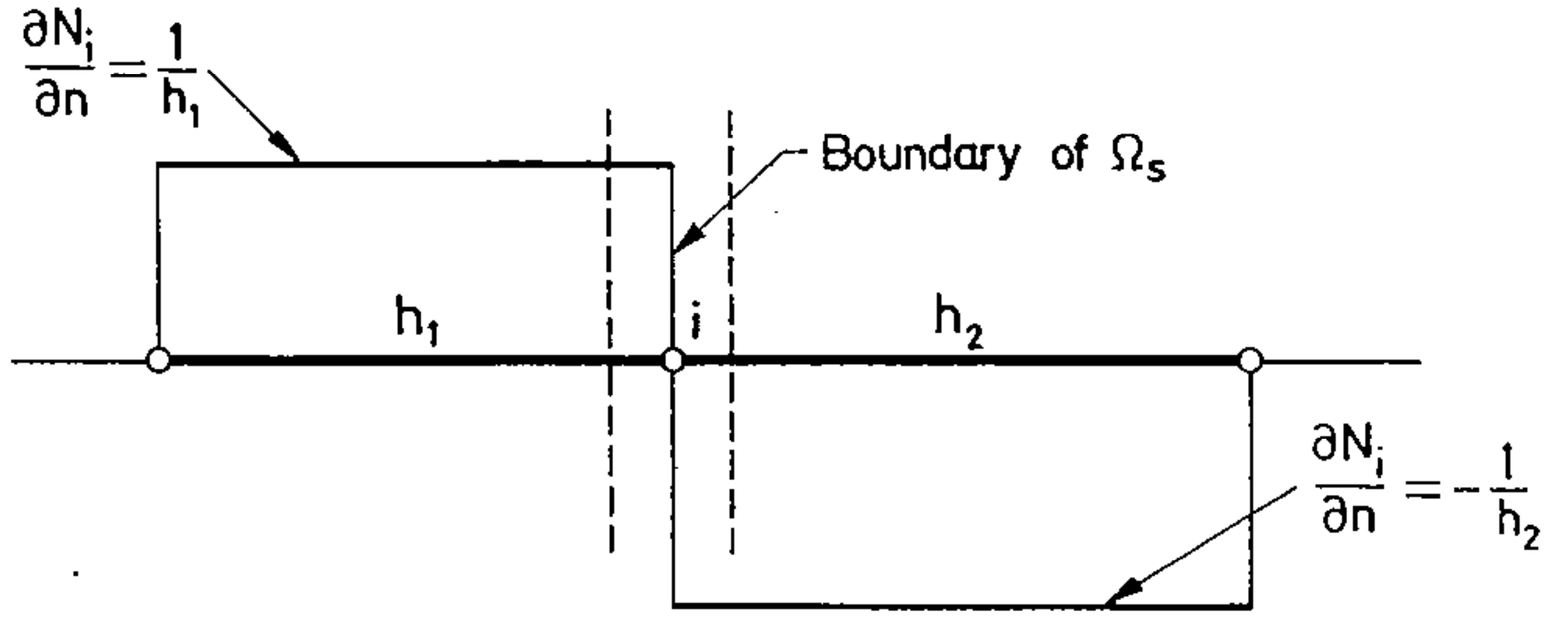

Figure 3. Discontinuity of gradient at boundaries of control volume.

The theory of *distributions* indicates that the jump in $\frac{\partial \hat{u}}{\partial n}$ accros the boundary should be given the average value (though of course in a finite sense position either inside or outside the jump could be justified). It will indeed be found that the mid position is optimal and the value should be then

$$\frac{\partial \hat{u}}{\partial n} = \frac{1}{2}\left(\left.\frac{\partial \hat{u}}{\partial n}\right|_1 + \left.\frac{\partial \hat{u}}{\partial n}\right|_2 \right) \tag{14}$$

where $\left.\frac{\partial \hat{u}}{\partial n}\right|_1$ and $\left.\frac{\partial \hat{u}}{\partial n}\right|_2$ are respectively the values of $\frac{\partial \hat{u}}{\partial n}$ over elements 1 and 2 sharing the interface under consideration.

An illustration of both finite element and finite element approximations can be easily obtained in a one dimensional example of Figure 4 where equal element of size h are used.

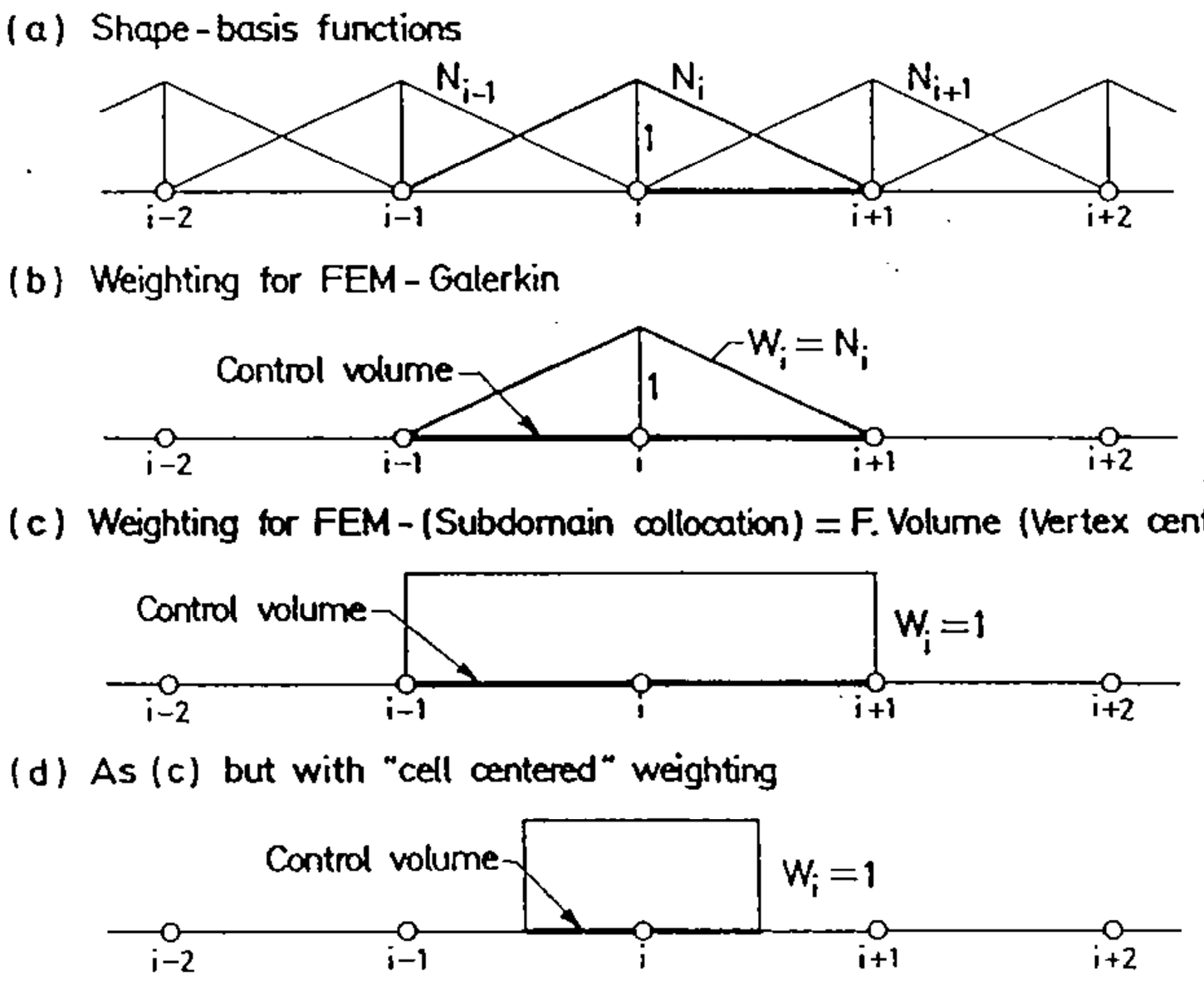

Figure 4. A one dimensional problem.

With linear shape functions used the finite element (Galerkin) approximation to eqs.(10), with $A_i = A = const.$, $Q = Q(x)$, we have a typical assembled equation (which can be easily verified after addition of approximate integrals)

$$\left[\frac{h}{6}\dot{u}_{i+1} + \frac{2h}{3}\dot{u}_i + \frac{h}{6}\dot{u}_{i-1}\right] + \frac{A}{2}[u_{i+1} - u_{i-1}] - \left[\frac{k}{h}u_{i+1} - \frac{2k}{h}u_i + \frac{k}{h}u_{i-1}\right] - f_i = 0 \tag{15}$$

where

$$f_i = \int_{-h}^{h} N_i Q dx \tag{16}$$

The corresponding finite volume equation is obtained using the approximation (14), as

$$\left[\frac{h}{2}\dot{u}_{i+1} + h\dot{u}_i + \frac{h}{2}\dot{u}_{i-1}\right] + A[u_{i+1} - u_{i-1}] - \left[\frac{k}{2h}u_{i+2} - \frac{k}{h}u_i + \frac{k}{2h}u_{i-2}\right] - \bar{f}_i = 0 \tag{17}$$

where

$$\bar{f}_i = \int_{-h}^{h} Q dx \tag{18}$$

It can be easily noted that the two approximations are similar but by no means identical.

The finite volume considered has doubled the mass contained in the finite element. The force f_i is also doubled in case of a constant Q. Further, the mass is not distributed in same proportion at the nodes and neither is the "force" when $Q = Q(x)$.

As expected the convective terms are exactly the double of those obtained by the finite element procedure.

Diffusion now is approximated using external nodes and indeed it is readily recognized that its value is represented by a (curvature) approximation for a mesh of double the size.

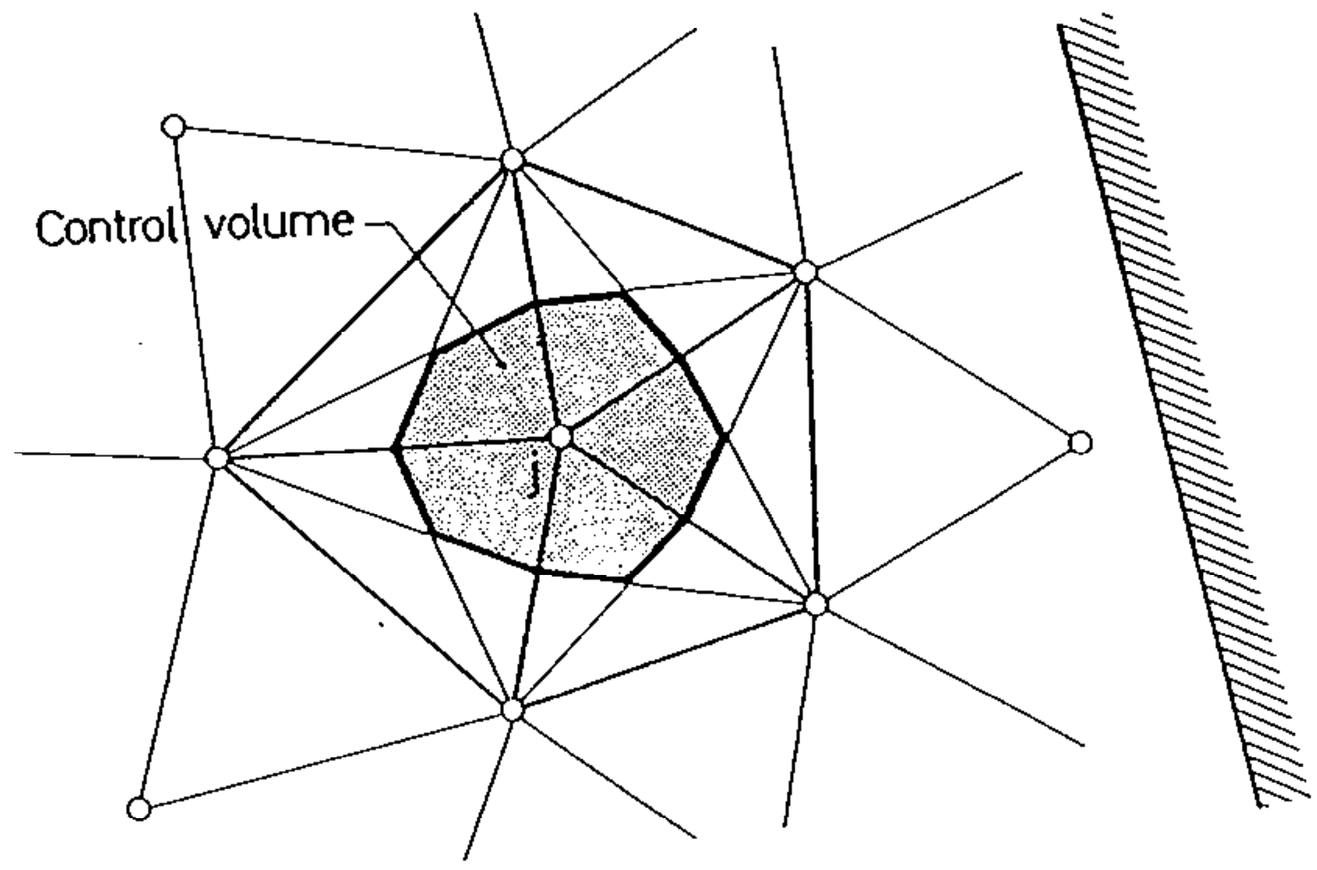

Figure 5. Cell centered control volume.

In the preceeding we have tried to provide "weigthing areas"or control volumes coinciding with elements. Clearly this presents a difficulty and we can now realize why many finite volume methods are applied in so called *cell centered* schemes. Thus if we consider again the discretization of Figure 1 we can, as in Figure 5, assign a control volume to each node without overlapping of the weighted area (the obvious division of each triangle is now indicated). In Figure 4 we show the one dimensional equivalent of above and the reader can readily verify that the finite volume equation now becomes

$$\left[\frac{h}{8}\dot{u}_{i+1} + \frac{6h}{8}\dot{u}_i + \frac{h}{8}\dot{u}_{i-1}\right] + \frac{A}{2}[u_{i+1} - u_{i-1}] - \left[\frac{k}{h}u_{i+1} - \frac{2k}{h}u_i + \frac{k}{h}u_{i-1}\right] - \bar{f}_i = 0 \quad (19)$$

This has the same conectivity as the finite element equations and indeed retrieves here exactly the convective and diffussive terms however showing as before different mass and force distributions (note that now $\bar{f}_i = \int_{-h/2}^{+h/2} Q dx$).

Indeed one must remark here that the use of consistent mass forms which is found to be beneficious in transient Euler fluid dynamics computations using the finite element approximation has never found its way into the finite volume way of thinking. Here the users invariably lump the masses implying for instance in the 1–D example that

$$\dot{u}_{i-1} = \dot{u}_i = \dot{u}_{i+1} \quad (20)$$

If such lumping is done both approximations are identical.

A Quantitative Example

To illustrate the applicability and perfomance of finite volume methods we shall consider a single example of an axially loaded elastic bar of lenght $2l$ (Figure 6). The axial load q will be taken either

as constant

Case I $q = \text{const.}$

or linear

Case II $q = cx$

The equilibrium equation and the boundary conditions read now

$$\begin{aligned} &\frac{\partial}{\partial x}\left(EA\frac{\partial u}{\partial x}\right) + q = 0 \qquad 0 \le x \le 2l \\ &u = 0 \quad \text{in} \quad x = 0 \\ &P = EA\frac{\partial u}{\partial x} = 0 \quad \text{in} \quad x = 2l \end{aligned} \quad (21)$$

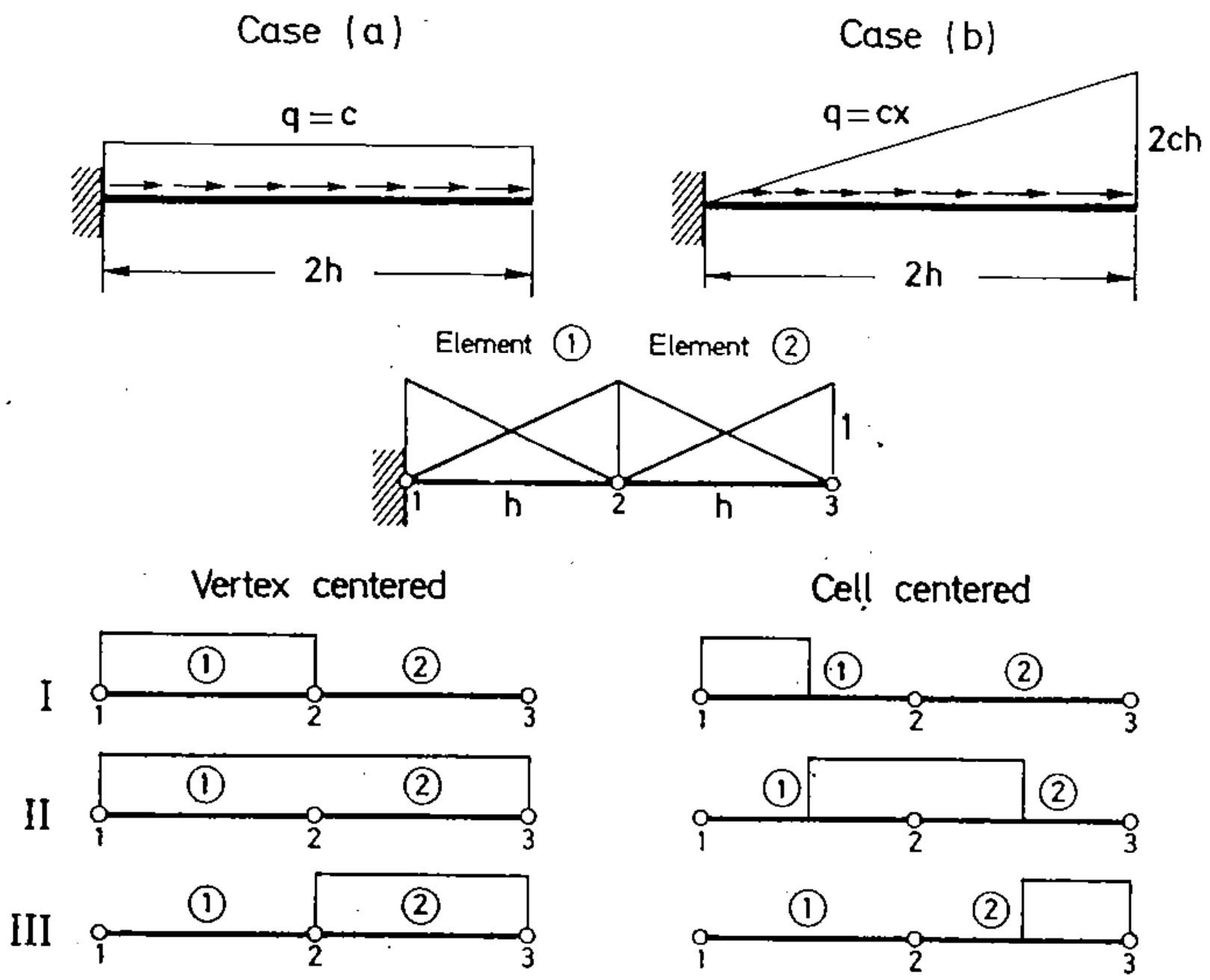

Figure 6. Elastic bar under axial load.

In above u is the axial displacement, P the axial force and E and A are the Young modulus and the area of the bar transverse cross section, respectively.

Following the arguments of proceeding section a typical finite volume equation can be written as

$$\left[EA\frac{\partial u}{\partial x}\right]_R - \left[EA\frac{\partial u}{\partial x}\right]_L + \int_{l_v} q dx = 0 \tag{22}$$

where L and R stand for left and right ends of *volume* of the lenght l_v.

Next we discretize the bar in three two node elements of equal size h. Inside each element the displacements u are linearly interpolated as

$$u = \sum_{i=1}^{2} N_i^{(e)} u_i^{(e)} \tag{23}$$

with $N_i^{(e)} = \frac{1}{2}(1 + \xi\xi_i)$ being the standard linear shape functions of the element.

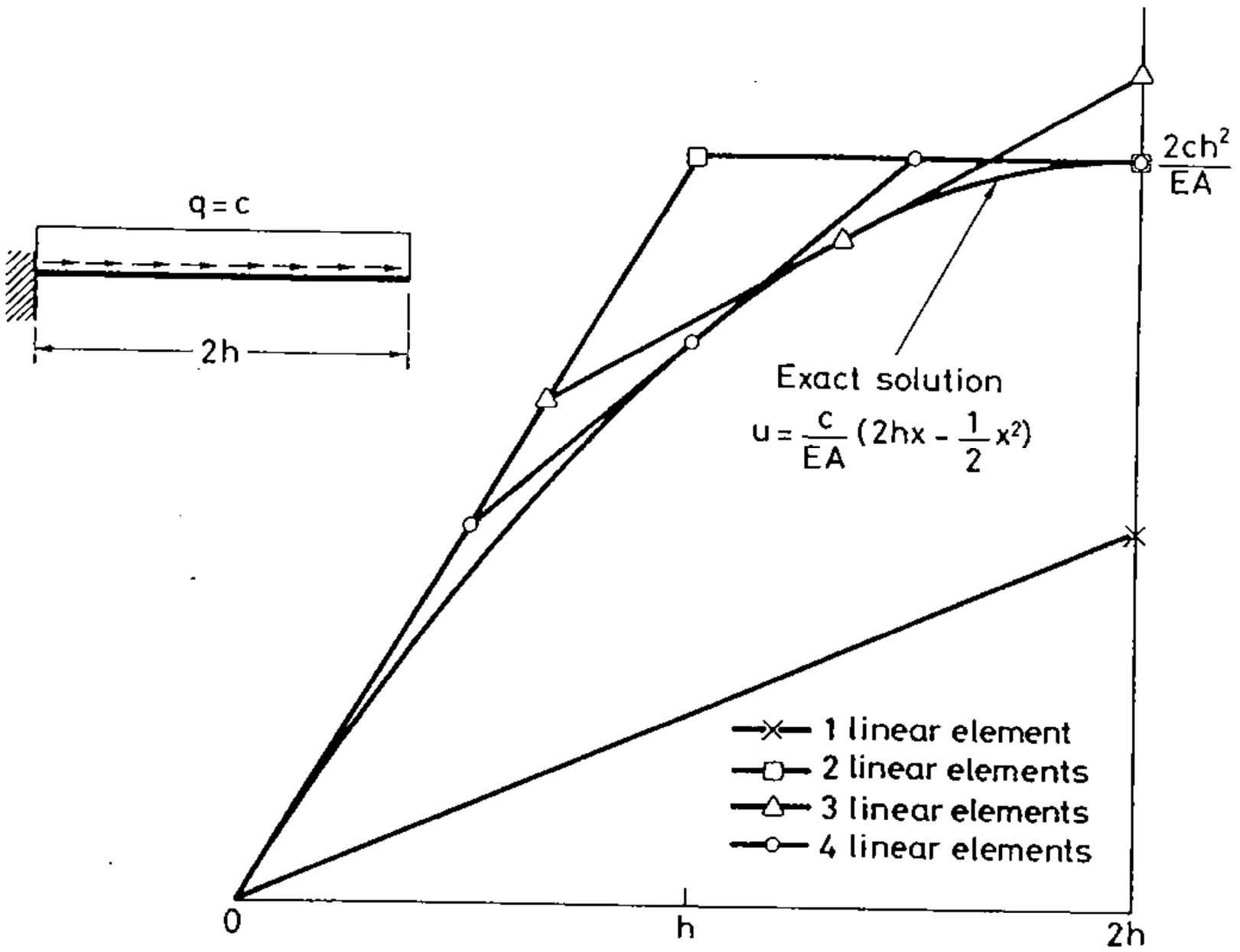

Note: the finite element and cell centered solutions give exact nodal results in all cases

Figure 7. Axially loaded bar. Convervenge of vertex centered finite volume solutions for meshes of 1, 2, 3 and 4 linear elements.

Mesh	Node	Vertex centered		Cell Centered
		Displacement formulation	Mixed formulation	Displacement formulation
1 element	2	50%	25%	12.5%
2 elements	2	9.09%	4.54%	2.27%
	3	12.5%	6.22%	3.5 %
3 elements	2	3.89%	1.85%	1.03%
	3	4.37%	2.14%	1.11%
	4	5.58%	2.77%	1.41%

Note: The finite element solution gives exact nodal results in all cases

Table I. Bar under linearly varying axial load. Percentage errors in nodal displacements for different meshes of linear elements using vertex centered and cell centered finite volume schemes.

Concluding Remarks

From eq.(17) it is easy to observe that for the first order (gradient) terms the approximations given by the vertex centered finite volume process can be readily confined to element assemblies and that evaluations of the approximation coefficients on interfaces can be efficient. The approximation is either similar or identical to that of finite elements and can be extended to higher order interpolations without difficulty. Figure 8 shows some possibilities.

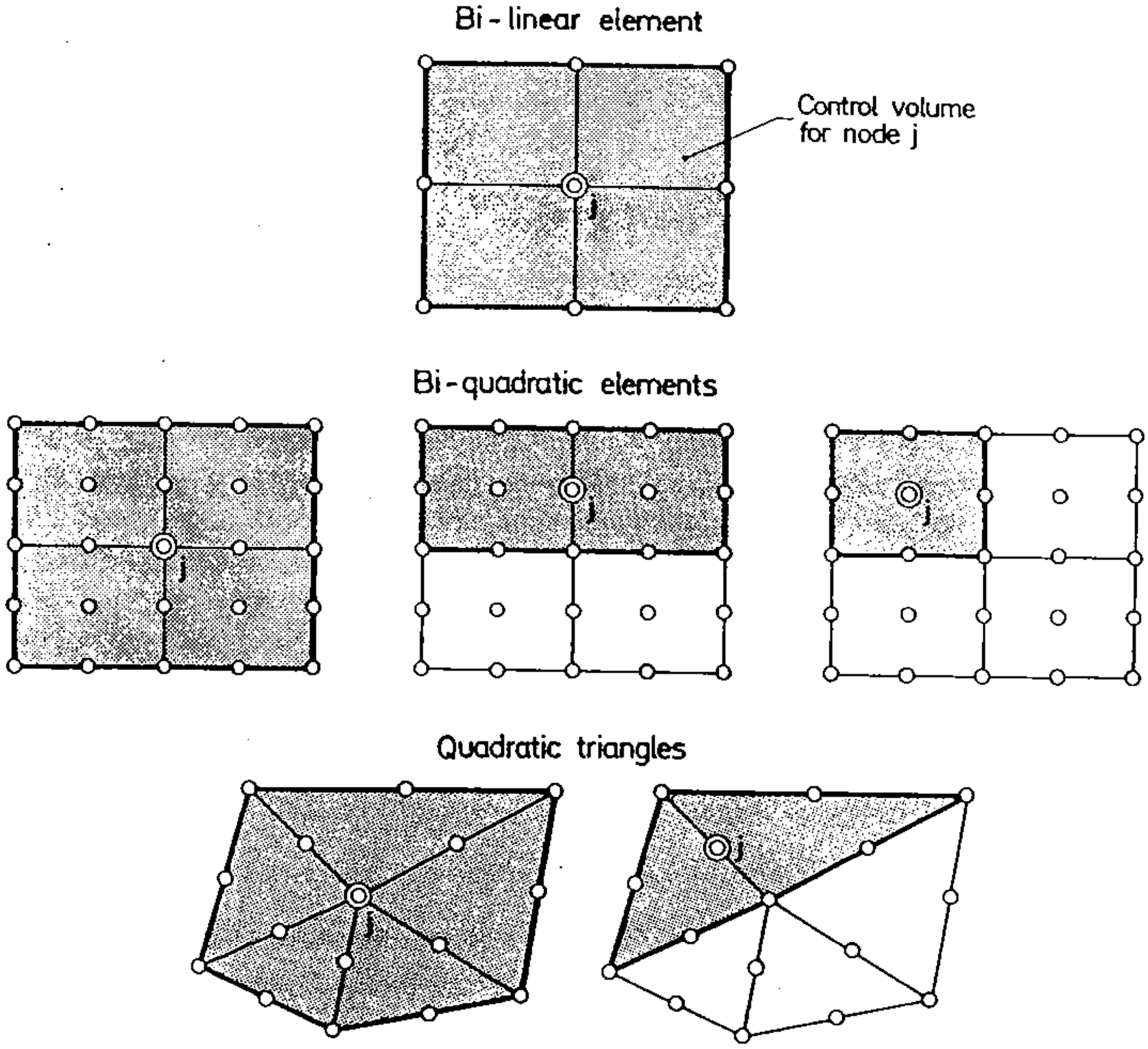

Figure 8. Control volumes for node j for higher order interpolations using quadrilateral and triangular meshes.

This type of approximation does not lend itself simply to second order (diffusion) terms as it involves a wide band of nodes (see Figure 9). This is however possible if explicit, iterative solution methods are used

The problem can be resolved by avoiding second order derivatives by using mixed equation systems. To illustrate the last possibility we shall consider only the diffusive term only in the one dimensional equivalent of eq.(10). writting the relevant equations as

$$\frac{\partial q_i}{\partial x_i} - Q = 0$$

$$q_i + k\frac{\partial u}{\partial x_i} = 0$$

CASE I, $q = c$

Application of eq.(22) toghether with interpolation (23) to the three volume domains surrounding nodes 1 (element 1), node 2 (element 1 and 2) and node 3 (element 3) gives (taking into account eq.(14))

Volume 1: Element 1

$$\frac{EA}{h}\left[\frac{u_1}{2} + u_2 - \frac{u_3}{2}\right] = ch$$

Volume 2: Elements 1+2

$$\frac{EA}{h}[u_2 - u_1] = 2ch$$

Volume 3: Element 3

$$\frac{EA}{2h}[u_3 - u_1] = ch$$

Note that for volumes 2 and 3 the boundary condition on the traction free end has been imposed exactly.

Solution of above system (with $u_1 = 0$) yields

$$u_2 = u_3 = \frac{2ch^2}{EA}$$

Figure 7 shows the convergence of the vertex centered finite volume solution for meshes of 1, 2, 3 and 4 elements respectively.

It can be easily checked that the finite element and the cell centered solutions for this case are identical and give the exact solution at nodes in all meshes.

CASE II, $q = cx$

Table I shows the percentage error of the vertex centered solution for the nodal axial displacement using three meshes of 1,2 and 3 elements. Note the big error (50%) in the end displacement obtained with the one element mesh. This error reduces to 5.158% if 3 elements are used.

The cell centered solution differs in this case from the nodaly exact finite element values due to the difference in the nodal load (force) vectors as previously explained. Percentage errors in the nodal displacement for the cell centered case are also presented in last column of Table I and show improvement with respect to the vertex centered solution.

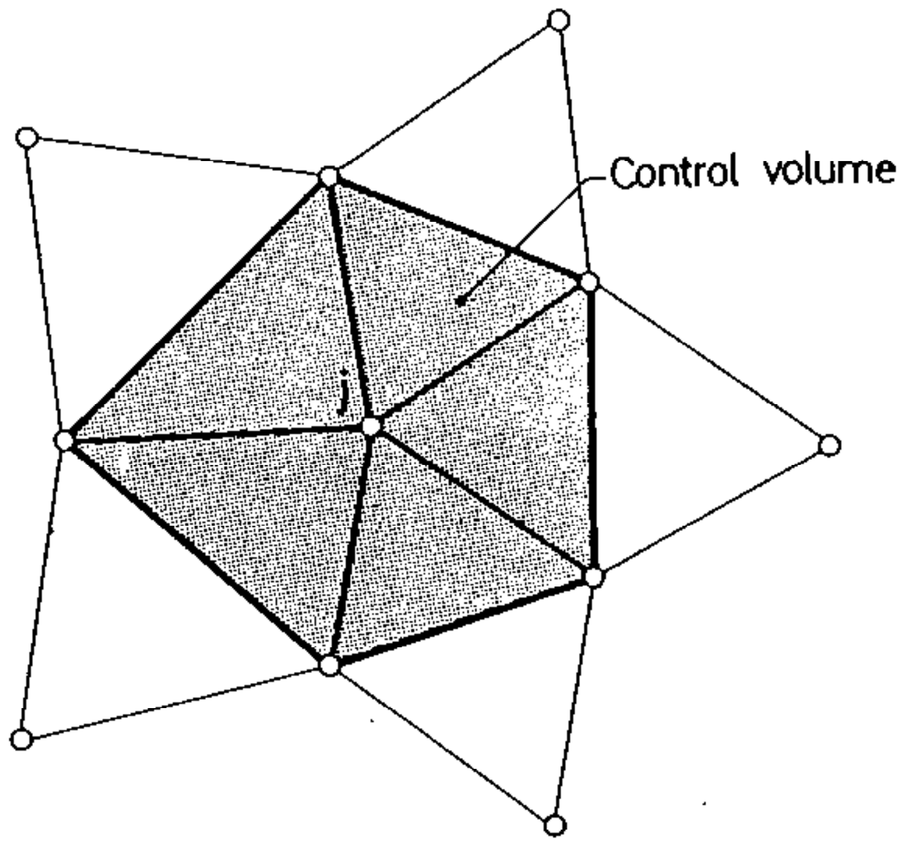

Figure 9. Nodes involved in the discretized equation of an arbitrary control volume using the vertex centered scheme and a "displacement" formulation.

Now with a mixed approximation each of the volumes can be treated as before involving only integration over Ω_j for each assembly. The procedure is simple and could readily be used in many applications in which continuous variation of q_i and u can be assumed with the corresponding gain in accuracy as shown in the elastic bar example given in the Appendix. Here excellent accuracy is obtained and results for the two load cases considered are again shown in Figure 7 and Table I.

Extension of above ideas to various elasticity and plate problems can be easily envisaged and it will be shown that very simple *elements* with simply assembly form can be derived avoiding such difficulties as mechanism formation, etc. inherent in reduced integration procedures frequently used in practice . We shall show such examples elsewhere.

References

[1] Mac Donald, P.W. "The computation of transonic flow through two dimensional gas turbine cascades", *ASME* paper 71-GT-89, (1971).

[2] MacCormack, R.W. and Paullay, A.J. "Computational Efficiency achieved by time splitting of finite difference operators", *AIAA* paper 72–154, San Diego, (1972).

[3] Rizzi, A.W. and Inouye, M. "Time split finite volume method for three dimensional blunt-body flows", *AIAA Journal*, 11, 1478–85, (1973).

[4] Patankar, S.V., "*Numerical heat transfer and fluid flow*", Series in Computational Methods in Mechanics and Thermal Sciences, W.J. Minkowycz and E. M. Sparrow (Eds.), Hemisphere Publising Corp., (1980).

[5] Wilkins, M.L. "Calculations of elasto-plastic flow". *Methods of Computational Physics* (Eds. B.alder et al.), Vol. 3, Academic Press, (1964).

[6] Hirsch, C. "*Numerical computation of internal and external flow*", Vol. I, J. Wiley, (1989).

[7] Zienkiewicz, O.C. and Taylor, R.L. "*The finite element method*", Vol. I. Mc Graw Hill, (1989).

APPENDIX

Finite volume solutions for the bar problem of Figure 6 using a mixed approximation

We consider the bar equilibrium equations written as

$$\begin{aligned} &\frac{dP}{dx} + q = 0 \\ &P - EA\frac{du}{dx} = 0 \qquad \text{in} \quad 0 \leq x \leq 2l \end{aligned} \tag{A.1}$$

with boundary conditions

$$\begin{aligned} &u = 0 \quad \text{in} \quad x = 0 \\ &P = \bar{P} \quad \text{in} \quad x = 2l \end{aligned} \tag{A.2}$$

The weighted residual form of eqs.$(A.1)$ reads

$$\begin{aligned} &\int_0^{2l} W \left[\frac{dP}{dx} + q\right] dx = 0 \\ &\int_0^{2l} \bar{W} \left[P - EA\frac{du}{dx}\right] dx = 0 \end{aligned} \tag{A.3}$$

Choossing $W = \bar{W} = 1$ inside each computation domain of lenght l_v we obtain, after adequate integration by parts,

$$\begin{aligned} &P_R - P_L + \int_{l_v} q dx = 0 \\ &\int_{l_v} P dx - [EAu]_R + [EAu]_L = 0 \end{aligned} \tag{A.4}$$

where indexes R and L refer to right and left ends of the "finite volume" considered.

Next the bar is discretized in linear finite elements where a linear approximations of the axial force P and the displacement u is chosen as

$$P = \sum_{i=1}^{2} N_i^{(e)} P_i^{(e)} \qquad , \qquad u = \sum_{i=1}^{2} N_i^{(e)} u_i^{(e)} \tag{A.5}$$

Substitution of $(A.5)$ in $(A.9)$ yields the following system of equations for a single two-element domain linking nodes $i-1, i$ and $i+1$.

$$\boxed{\begin{aligned} &P_{i+1} - P_{i-1} + f_i = 0 \\ &\frac{h^{(i+1)}}{2}(P_i + P_{i-1}) + \frac{h^{(i)}}{2}(P_i + P_{i+1}) + EA(u_{i-1} - u_{i-1}) = 0 \end{aligned}} \tag{A.6}$$

Where $h^{(i-1)}$ and $h^{(i)}$ are the lenghts of the two elements considered and

$$f_i = \int_l q dx \qquad \text{with} \qquad l = h^{(i-1)} + h^{(i)} \tag{A.7}$$

Application of eqs.(A.6) to the bar problem of Figure 6 under uniformly distributed axial loading ($q = c$) yields for the two element mesh case:

Volume 1: Element 1

$$P_2 - P_1 + ch = 0$$
$$\frac{h}{2}(P_1 + P_2) + EA(u_1 - u_2) = 0$$

Volume 2: Elements 1+2

$$P_3 - P_1 + 2ch = 0$$
$$\frac{h}{2}(P_3 + 2P_2 + P_1) + EA(u_1 - u_3) = 0$$

Volume 3: Element 2

$$P_3 - P_2 + ch = 0$$
$$\frac{h}{2}(P_2 + P_3) + EA(u_2 - u_3) = 0$$

Solution of above six equations with $P_3 = u_1 = 0$ yields

$$u_2 = \frac{3ch^2}{2EA}, \quad u_3 = \frac{2ch^2}{EA}, \quad P_2 = ch, \quad P_1 = 2ch$$

which coincides precisely with the exact solution. The same preciseness is obtained for the 1 and 3 element meshes as shown in Figure 7.

Results for the linear loading case ($q = cx$) obtained with the mixed approximation are shown in Table I. Note the improvement in accuracy with respect the vertex centered displacement approach, although the cell centered scheme still yields the best approximation for this case.